

Rescattering for Extended Atomic Systems

Ulf Saalmann and Jan M. Rost

Max Planck Institute for the Physics of Complex Systems, Nöthnitzer Straße 38, 01187 Dresden, Germany
(Received 24 December 2007; published 4 April 2008)

Laser-driven rescattering of electrons is the basis of many strong-field phenomena in atoms and molecules. Here, we will show how this mechanism operates in extended atomic systems, giving rise to effective energy absorption. Rescattering from extended systems can also lead to energy loss, which in its extreme form results in nonlinear light-induced trapping. Intense-laser interaction with atomic clusters is discussed as an example. We explain fast electron emission, seen in experimental and numerically obtained spectra, by rescattering of electrons at the highly charged cluster.

DOI: 10.1103/PhysRevLett.100.133006

PACS numbers: 33.80.Rv, 36.40.Wa, 52.20.Fs, 64.60.an

Laser-driven rescattering of electrons [1,2] is at the heart of strong-field atomic physics. The basic principle is very simple [1]: a bound electron is released from an atom (or a negative ion [3]) with the help of the strong electric field of a laser, by which it is subsequently driven back to the ion. On return to the ion the electron may recombine (emitting harmonic radiation [4] with the access to attosecond laser pulses [5]), ionize other electrons (inducing multiple ionization [6]), or may be backscattered (gaining high kinetic energy termed above-threshold ionization [7]). Because of the strong dependence of the tunnel probability on the field the release time is restricted to phases of the laser period with maximal electric field. In the following we concentrate on linearly polarized light which exhibits the most pronounced rescattering effects.

Most direct evidence for the rescattering mechanism comes from measuring kinetic energies of the released electrons [8–11]. The momentum p an electron can acquire in an oscillating field $f(t) = F \cos(\omega t)$ of strength F and frequency ω depends on the phase $\varphi_0 = \omega t_0$ at the time t_0 of its release. At this time the vector potential of the field is $A_0 := A \sin \varphi_0 \equiv (F/\omega) \sin \varphi_0$ and this is exactly the momentum acquired, $p = A_0$. (We use atomic units.) Obviously, the maximum $p_{\max} = A \equiv F/\omega$ occurs at $\varphi_0 = \pi/2$ and results in a kinetic energy $E_{\max} = 2E_{\text{pond}}$ with the ponderomotive energy $E_{\text{pond}} := F^2/4\omega^2$. However, electrons with such high energies are rare [9] since they must be released from the atom when the electric field vanishes, which is very unlikely (see above). Electrons with energies even beyond $2E_{\text{pond}}$ are indicative for rescattering of electrons previously released.

For atoms the rescattering process can be understood in classical terms by an electron elastically [12] scattered at a zero-range potential in the presence of an electromagnetic field [13]; neglecting the Coulomb tail turned out to be of minor importance. In this case, and more generally, if the scattering time is much shorter than the laser period, the absorbed energy ΔE is given by [14]

$$\Delta E = 2\Delta\mathbf{p} \cdot \mathbf{A}(t') \quad (1)$$

with $\Delta\mathbf{p}$ the momentum change at the time t' of scattering.

The absorption is particularly effective for a large momentum change $\Delta\mathbf{p}$, which is achieved through backscattering, and for scattering events taking place at a maximal vector potential (minimal electric field).

For an extended scattering potential we will see that optimum energy absorption upon rescattering requires completely different conditions, namely, forward scattering at maximal electric field.

This becomes obvious by analyzing the simplest situation of scattering from an extended potential. It can be realized with an electron passing under the influence of an oscillating electric field centrally a spherical well. The one-dimensional problem is sketched in Fig. 1. Assuming a constant potential $-V < 0$ inside the extended scatterer naturally generalizes the zero-range potential used in the context of rescattering at atoms [13]. Note that similar to the discussion before Eq. (1) for atoms, the time of crossing the potential boundaries may be assumed to be short compared to the laser period. Therefore, the boundaries are

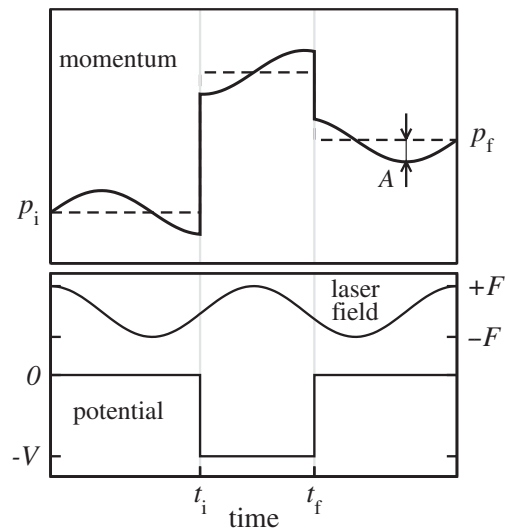


FIG. 1. Schematic picture of the scattering process. The upper part shows the electron's momentum, the lower part the potential and the value of the electric field (assumed to be homogeneous in space) as a function of time, respectively.

idealized here as steps in the potential. This allows for the corresponding electron dynamics to be solved analytically. The electron momentum

$$P_\alpha = p_\alpha + (F/\omega) \cos(\omega t) \quad (2)$$

contains a constant drift p_α (shown by dashed lines in Fig. 1) and an oscillating part due to the laser field (shown by thick solid lines in Fig. 1). In order to conserve energy across the boundaries of the potential reached at times t_i and t_f , respectively, the electron momentum must jump at those times.

The motion is determined by the laser (with field strength F and frequency ω), the potential (with width L and depth V), and the initial drift momentum p_i , cf. Fig. 1. A given entrance time t_i (or phase $\varphi_i := \omega t_i$) fixes the exit time t_f and phase $\varphi_f := \omega t_f$. Then the final momentum cf. Eq. (2), reads

$$P_f = [(A_f - A_i + \sqrt{P_i^2 + p^2})^2 - p^2]^{1/2}, \quad (3)$$

whereby the phases φ_i and φ_f are connected by

$$L\omega = (-A_i + \sqrt{P_i^2 + p^2})(\varphi_f - \varphi_i) - (A'_f - A'_i). \quad (4)$$

In addition to $A_\alpha = A \sin \varphi_\alpha$, we have defined $A'_\alpha := A \cos \varphi_\alpha$. The ‘‘transit’’ momentum $p := \sqrt{2V}$ characterizes the depth of the potential. We assume $p_i \geq A$ to guarantee monotonic motion of the electron and avoid multiple passing of the potential border.

The final momentum p_f cannot be expressed explicitly in terms of φ_i since Eq. (4) is essentially nonalgebraic. However, it is instructive to optimize p_f with respect to φ_i and φ_f . Then, Eq. (4) reveals the optimum width of the potential for extremal energy absorption under given laser light. One obtains extrema for $\varphi_{i,f} = \pm \pi/2 \bmod 2\pi$ and the maximum p_f for $\varphi_i = -\pi/2$ and $\varphi_f = +\pi/2$ with the electron passing the center of the potential at times between $-\pi/\omega$ and $+\pi/\omega$. Electron momentum and potential width read

$$p_{f,\max} = -A + [(2A + \sqrt{(p_i - A)^2 + p^2})^2 - p^2]^{1/2}, \quad (5)$$

$$L_{\max} = \frac{\pi}{\omega} (A + \sqrt{(p_i - A)^2 + p^2}). \quad (6)$$

In the limit of a deep potential, i.e., $p \gg p_i$ and $p \gg A$, both expressions simplify to

$$p_{f,\max} \approx 2\sqrt{Ap}, \quad (7)$$

$$L_{\max} \approx p \frac{\pi}{\omega}. \quad (8)$$

Obviously the optimal potential width L in Eq. (8) corresponds to the distance an electron travels with momentum p during half a cycle π/ω of the laser pulse [15].

At optimal width L_{\max} the maximum electron momentum achievable depends on both the laser field amplitude A and the depth of the potential [through p in Eq. (7)]. This is different from above-threshold ionization of single atoms where the maximal electron momentum is determined by the laser field only, namely $p_{\max} = \sqrt{5}A$ (or $E_{\text{kin,max}} = 10E_{\text{pond}}$) [7]. It should be mentioned that electrons with such high energies are typically a few orders of magnitude less abundant than low-energy electrons [10,16].

The energy absorption is maximized by an increased momentum during one half cycle of the pulse. In a full laser cycle a free electron absorbs as much energy as it loses. If, however, the drift momentum is increased by p for just one half of the cycle there is a net energy absorption. Using Eq. (2) it is given by

$$\Delta E = \int f(t)P(t)dt = Fp \int_{-\pi/2\omega}^{+\pi/2\omega} \cos(\omega t)dt = 2Ap, \quad (9)$$

in accordance with the result in Eq. (7). Whereas the absolute change of the momentum in the field, being $2A$, is independent of the drift momentum p the change of the kinetic energy Eq. (9) is proportional to it. Rewritten in terms of energies, we obtain for the maximum energy gain through rescattering from extended systems the central result of this Letter:

$$\Delta E = 4\sqrt{E_{\text{pond}}}\sqrt{V}. \quad (10)$$

The acceleration of the electrons depends on both, the laser field strength A and the depth V of the scattering potential. Interestingly, this situation is akin to the so-called powered swing-by (or gravity-assisted maneuver) of spacecrafts [17]. There, thrust for accelerating, decelerating, or redirecting the spacecraft is applied only for short intervals of time and not in an oscillatory fashion as in the case of a laser. However, similar to the situation considered here, thrust is most effectively applied when the space craft has high momentum, which is the case at the periapsis of a swing-by at a planet.

As mentioned before, for a given potential the phases φ_i and φ_f are linked through Eq. (4). For the case of deep potentials, when $p \gg p_i$ and $p \gg A$, this equation simplifies to $L\omega \approx p(\varphi_f - \varphi_i)$. This fixes the difference of the phases and one may write the momentum explicitly as $p_f(\varphi) = 2[Ap \cos(\varphi/2) \sin(L\omega/2p)]^{1/2}$ with $\varphi := \varphi_f + \varphi_i$ the only parameter left for optimizing p_f . For $\varphi = 0$, i.e., when φ_i and φ_f are symmetric with respect to the field maximum, the momentum reads

$$p_f = p_{f,\max} \left[\sin\left(\frac{\pi}{2} \frac{L}{L_{\max}}\right) \right]^{1/2}, \quad (11)$$

with the maximal momentum from Eq. (7) and the optimal system width L_{\max} from Eq. (8).

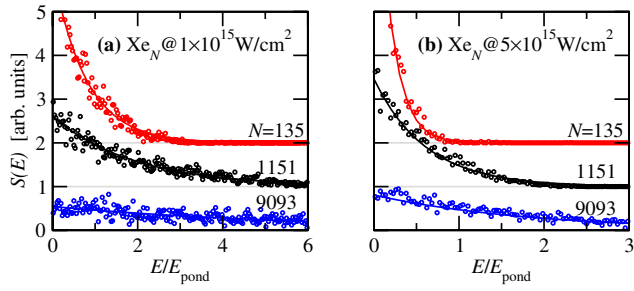


FIG. 2 (color online). Kinetic energy distribution of electrons $S(E)$, i.e., number of electrons with an energy between $E - \delta E/2$ and $E + \delta E/2$ whereby $\delta E = 0.03E_{\text{pond}}$, for two laser pulses of 400 fs duration (full width at half maximum of a Gaussian pulse) and peak intensities of 1×10^{15} W/cm² (a) and 5×10^{15} W/cm² (b), respectively. Shown are the results for three different cluster sizes Xe₁₃₅, Xe₁₁₅₁, and Xe₉₀₉₃, respectively. The first two are shifted upwards for better visibility. Each set of points is fitted (solid lines) by an exponential curve according to Eq. (12). Note that the energy scale is given by the corresponding ponderomotive energy E_{pond} .

To illustrate the relevance of the rescattering mechanism in extended systems we present in the following results of microscopic calculations for rare-gas cluster exposed to intense-laser radiation [18]. The theoretical approach describes the laser-driven electronic nanoplasma and the ionic explosion dynamics by means of classical equations of motion. It has been successfully applied to study, e.g., absorption mechanisms for a wide range of clusters sizes and laser pulses by various groups [19–22]. Figure 2 shows kinetic energy distributions of electrons $S(E)$ as obtained for xenon clusters of different sizes and various laser pulse parameters. The calculations are rather expensive since the electrons have to be propagated for a long time (typically a few picoseconds) in order to obtain converged results for their final kinetic energy, which otherwise would be spoiled by the large, long-range, and time-dependent attractive potential of the exploding cluster. All distributions show an exponential behavior in accordance with observations from experiments for somewhat larger xenon clusters [23,24] as well as silver cluster of similar size [25]. Fitting an exponential function,

$$S(E) = C \exp(-E/E_{\text{kin}}) \quad (12)$$

to these distributions yields the decay parameter E_{kin} and the irrelevant normalization parameter C . The parameters E_{kin} , which are listed in Table I, strongly depend on the cluster size and the laser pulse, but reveal a clear trend: The larger the cluster the faster the emitted electrons. This trend originates in the deeper potential for larger clusters, i.e., larger V in Eq. (10), which leads to a stronger acceleration at rescattering.

Note that the energy can exceed the ponderomotive energy considerably as seen, in particular, for the largest cluster Xe₉₀₉₃. Knowing the cluster potential from the

TABLE I. Electron energies in units of the ponderomotive energy E_{pond} from xenon clusters of three sizes and two different laser pulses. The exponential fit parameter E_{kin} from the microscopic calculations shown in Fig. 2 are compared to the value ΔE of the rescattering model in Eq. (10).

Cluster size N	135		1151		9093	
Laser pulse	(a)	(b)	(a)	(b)	(a)	(b)
Microscopic result $E_{\text{kin}}/E_{\text{pond}}$	0.78	0.27	1.98	0.60	5.43	1.74
Rescattering model $\Delta E/E_{\text{pond}}$	0.19	0.09	1.53	0.65	3.68	1.58

simulation [26] we can estimate the electron energies with the rescattering model of Eq. (10) and list them for comparison in Table I. They agree surprisingly well considering the simplicity of the model and the fact that the electron spectrum of the microscopic calculations (Fig. 2) contains also all electrons released directly. We attribute the agreement to the fact that the exponential tail is due to the fast electrons which are dominantly emitted by rescattering. Additionally, most of the electrons are ejected at the resonance of the cluster [24,25] where the acceleration is optimal. This is certainly not the case for the smallest cluster, Xe₁₃₅, considered here. It is almost completely disintegrated at the time when the laser pulse reaches its peak. What we assume to determine the parameters for rescattering is therefore not valid and consequently poor is the quantitative prediction of the electron spectrum by rescattering for this cluster.

Similar to the calculated electron energy distributions $S(E)$ experimental spectra can be characterized by constants E_{kin} quantifying the exponential decay. They are shown for measurements [25,27] of various clusters along with the theoretical results discussed above in Fig. 3. Clearly, they are larger than the ponderomotive energy, i.e., above the dashed line in Fig. 3. Note that corresponding data for atoms [10] are below this line. Even in cases

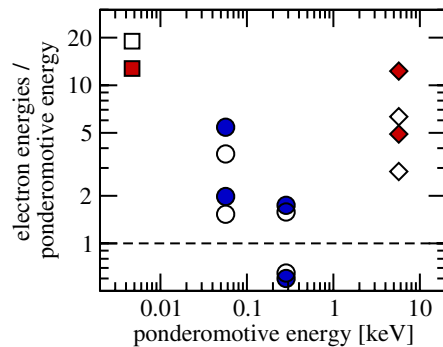


FIG. 3 (color online). Electron energies as a function of the ponderomotive energy E_{pond} from various clusters. The solid symbols show E_{kin} for experiments (red or gray) and microscopic calculations (blue or dark gray): Ag₁₀₀₀ (square, [25]), Ar₁₇₀₀ and Ar₃₃₀₀₀ (diamonds, [27]), Xe₁₁₅₁ and Xe₉₀₉₃ (circles, Fig. 2). The corresponding estimates ΔE from the rescattering model (10) are shown by open symbols.

where one observes a plateau energetic electrons from atoms are much less likely than for extended systems such as clusters.

In contrast to the microscopic calculation we generally neither know the charge nor the radius of the cluster at the peak of the laser pulse. However, there are two exceptions: (i) the pulse is very short [27] or (ii) the delay of a dual pulse is adjusted to induce resonant ionization [25]. In both cases one can roughly estimate the unknown cluster parameters which determine width L and depth V of the extended potential for rescattering. In case (i) one can neglect the cluster expansion, the radius of the scattering potential is the initial cluster radius R . The charge Q can be estimated from a simple over-the-barrier model $Q = FR^2$ [28]. Hence, with the potential depth $V = 3Q/2R$ of a homogeneously charged sphere we can by means of Eq. (10) determine the electron energies (open diamonds in Fig. 3) in reasonable agreement with the experimental values. In particular the ratio between the larger and the smaller cluster size is well reproduced. Note that the experimental signal is a sum over clusters of different size and the laser focus. This may be crucial [29] and agreement with a simple model on the absolute scale cannot be expected. For case (ii) we assume that the cluster expands homogeneously over the delay between the (short) double pulses. Thus one has at resonance $Q/R^3 \equiv \omega^2$ [22]. The charge Q can be roughly assessed from measured final ion charges [30]. Assuming an average ion charge of two we estimate a value (open square in Fig. 3) slightly above the experimental one.

The experimental and numerical examples of rare-gas clusters demonstrate that the simple rescattering mechanism for extended potentials we have introduced can provide considerable insight into complicated many-body dynamics as it occurs in these clusters including semi-quantitative predictions. However, the analytical results from Eqs. (3) and (4) are far more general than the example of rare-gas clusters may suggest and should, e.g., also describe nonlinear absorption of laser energy in quantum dots. Moreover, rescattering in extended systems does not only provide conditions for optimum energy absorption from the light, it also answers the opposite question: Given a certain rescattering potential and laser pulse, what is the maximum velocity of a particle which can be brought to rest (remains sticking in the scattering system) under the combined action of laser and potential? This situation is also described by Eq. (5) if one interchanges the indices “ f ” and “ i ” and sets $p_f = 0$. The result is given by Eq. (7), but now $p_{i,\max} \approx 2\sqrt{Ap}$ stands

for the maximum initial momentum an electron can have and still will stick to the extended potential being most efficiently decelerated by the potential and the light. This constitutes nonlinear light-induced trapping in extended systems.

We acknowledge support from the Kavli Institute for Theoretical Physics (KITP) in Santa Barbara, where this work has been started.

-
- [1] P. B. Corkum, Phys. Rev. Lett. **71**, 1994 (1993).
 - [2] M. Yu. Kuchiev, JETP Lett. **45**, 404 (1987).
 - [3] M. V. Frolov *et al.*, J. Phys. B **38**, L375 (2005).
 - [4] M. Lewenstein *et al.*, Phys. Rev. A **49**, 2117 (1994).
 - [5] A. Scrinzi *et al.*, J. Phys. B **39**, R1 (2006).
 - [6] A. Becker, R. Dörner, and R. Moshhammer, J. Phys. B **38**, S753 (2005).
 - [7] D. B. Milosević *et al.*, J. Phys. B **39**, R203 (2006).
 - [8] P. Agostini *et al.*, Phys. Rev. Lett. **42**, 1127 (1979).
 - [9] P. B. Corkum, N. H. Burnett, and F. Brunel, Phys. Rev. Lett. **62**, 1259 (1989).
 - [10] G. G. Paulus *et al.*, Phys. Rev. Lett. **72**, 2851 (1994).
 - [11] B. Walker *et al.*, Phys. Rev. Lett. **77**, 5031 (1996).
 - [12] The collision with the potential itself is elastic, i.e., does not change the energy of the electron. It can, however, absorb energy from the time-dependent field.
 - [13] G. G. Paulus *et al.*, J. Phys. B **27**, L703 (1994).
 - [14] N. M. Kroll and K. M. Watson, Phys. Rev. A **8**, 804 (1973).
 - [15] T. Taguchi, T. M. Antonsen, Jr., and H. M. Milchberg, Phys. Rev. Lett. **92**, 205003 (2004).
 - [16] K. J. Schafer *et al.*, Phys. Rev. Lett. **70**, 1599 (1993).
 - [17] A. F. B. A. Prado, J. Guid. Control Dyn. **19**, 1142 (1996).
 - [18] U. Saalmann, C. Siedschlag, and J. M. Rost, J. Phys. B **39**, R39 (2006).
 - [19] C. Rose-Petrucci *et al.*, Phys. Rev. A **55**, 1182 (1997).
 - [20] I. Last and J. Jortner, Phys. Rev. A **62**, 013201 (2000).
 - [21] K. Ishikawa and T. Blenski, Phys. Rev. A **62**, 063204 (2000).
 - [22] U. Saalmann and J. M. Rost, Phys. Rev. Lett. **91**, 223401 (2003).
 - [23] E. Springate *et al.*, Phys. Rev. A **68**, 053201 (2003).
 - [24] V. Kumarappan, M. Krishnamurthy, and D. Mathur, Phys. Rev. A **67**, 043204 (2003).
 - [25] T. Fennel *et al.*, Phys. Rev. Lett. **98**, 143401 (2007).
 - [26] Since charge and radius of the cluster are time dependent we have chosen the values at the moment of the maximum charging rate, i.e., when most of the electrons are emitted.
 - [27] L. M. Chen *et al.*, Phys. Rev. E **66**, 025402(R) (2002).
 - [28] U. Saalmann, J. Mod. Opt. **53**, 173 (2006).
 - [29] M. R. Islam, U. Saalmann, and J. M. Rost, Phys. Rev. A **73**, 041201(R) (2006).
 - [30] T. Döppner *et al.*, Phys. Rev. Lett. **94**, 013401 (2005).